Accepted Manuscript

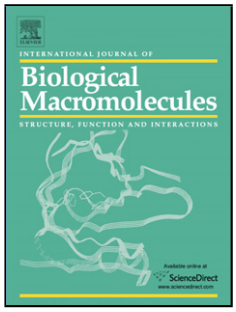

Title: Physicochemical Characterization of Water-Soluble Chitosan Derivatives with Singlet Oxygen Quenching and Antibacterial Capabilities

Authors: Noelia L. Vanden Braber, Ladislao I. Díaz Vergara, Faustino E. Morán Vieyra, Claudio D. Borsarelli, Mariana M. Yossen, Jorge R. Vega, Silvia G. Correa, Mariana A. Montenegro

PII: S0141-8130(16)32149-3
DOI: http://dx.doi.org/doi:10.1016/j.ijbiomac.2017.04.028
Reference: BIOMAC 7392

To appear in: *International Journal of Biological Macromolecules*

Received date: 24-10-2016
Revised date: 5-4-2017
Accepted date: 7-4-2017

Please cite this article as: Noelia L.Vanden Braber, Ladislao I.Díaz Vergara, Faustino E.Morán Vieyra, Claudio D.Borsarelli, Mariana M.Yossen, Jorge R.Vega, Silvia G.Correa, Mariana A.Montenegro, Physicochemical Characterization of Water-Soluble Chitosan Derivatives with Singlet Oxygen Quenching and Antibacterial Capabilities, International Journal of Biological Macromoleculeshttp://dx.doi.org/10.1016/j.ijbiomac.2017.04.028

International Journal of Biological Macromolecules

Physicochemical Characterization of Water-Soluble Chitosan Derivatives with Singlet Oxygen Quenching and Antibacterial Capabilities

Noelia L. Vanden Braber[1], Ladislao I. Díaz Vergara[1], Faustino E. Morán Vieyra[2], Claudio D. Borsarelli[2*], Mariana M. Yossen[3], Jorge R. Vega[3], Silvia G. Correa[4], Mariana A. Montenegro[1*]

[1] Centro de Investigaciones y Transferencia de Villa María (CITVM-CONICET-UNVM). Universidad Nacional de Villa María (UNVM). Campus Universitario, Arturo Jauretche 1555, Villa María, Córdoba, Argentina.

[2] Instituto de Bionanotecnología del NOA, (INBIONATEC). Universidad Nacional de Santiago del Estero (UNSE); CONICET. RN9, Km 1125, G4206XCP Santiago del Estero, Argentina.

[3] Instituto de Desarrollo Tecnológico para la Industria Química (INTEC-CONICET-UNL). Universidad Nacional del Litoral (UNL). Güemes 3450 (3000), Santa Fe, Argentina.

[4] Centro de Investigación en Bioquímica Clínica e Inmunología (CIBICI-CONICET-UNC), Universidad Nacional de Córdoba (UNC), Córdoba, Argentina.

*Corresponding authors:

mamontenegro03@yahoo.com.ar; Phone: +54-353-453-9100

cdborsarelli@gmail.com; Phone: +54-385- 423- 8352

Graphical Abstract

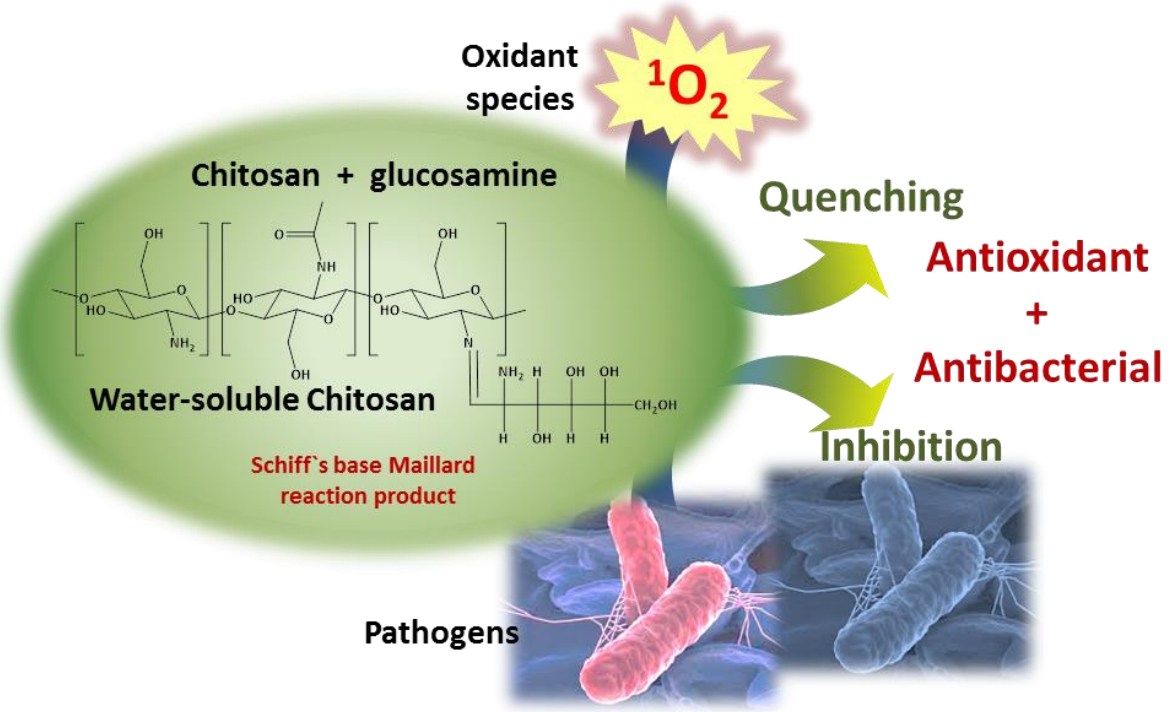

Highlights

- Water-soluble chitosan derivatives showed significantly larger solubility that the native Ch.
- Deacetylation degree (DD) of chitosan derivatives decreased by approximately 12%.
- Molecular weight of chitosan derivatives was reduced 6 times, suggesting the breakdown of the Ch chain.
- The singlet molecular oxygen quenching abilities of chitosan derivatives were proportional to DD of polysacharides.
- Water-soluble chitosan derivatives presented antimicrobial activity against pathogenic bacteria

ABSTRACT

New water-soluble chitosan derivatives (WSCh) were obtained by Maillard reaction (MR) between glucosamine (GA) with both low and medium molecular weight chitosans (Ch). The WSCh showed larger solubility than the respective Ch, while their deacetylation degree (DD) decreased by approximately 12 %. Infrared spectroscopy experiments of WSCh confirmed the formation of imine bonds after MR with intensified pyranose structure, and sugar molecules as polymer branches. However, a 6-times reduction of the molecular weight of WSCh was measured, indicating the breakdown of the polysaccharide chain during the MR. The polysaccharides quenched singlet molecular oxygen ($^1O_2$), with rate quenching constants correlating with the DD value of the samples, suggesting the important role of amino groups ($–NH_2$) in the deactivation of $^1O_2$. Additionally, all polysaccharides presented antimicrobial activity against pathogenic bacteria, e.g. *Staphylococcus aureus*, *Escherichia coli*, *Salmonella sp.*, *Enterococcus faecalis* and *Listeria ivanovii*, as tested by their minimum inhibitory concentration (MIC). This way we obtained new water-soluble polysaccharides, with similar functional properties to those presented by native Ch, enhancing its potential application as carrier material for bioactive compounds.

Keywords: water-soluble chitosans; singlet oxygen quenching; antimicrobial activity.

1. Introduction

Polysaccharides are the most abundant biopolymers in the biosphere, and for that reason and their biocompatibility are suitable for several applications, including nanotechnology [1]. Such is the case of chitin and chitosan (Ch), belonging to the family of natural amino-polysaccharides, which attracted significant scientific interest because of their biocompatibility, biodegradability and low toxicity [2,3]. Furthermore, Ch is a polysaccharide with immunostimulant, antimutagenic, anticancer, mucoadhesive, and antimicrobial properties; and it has been included into the generally recognized as safe (GRAS) list in the United States [4,5]. For all these features, Ch is widely used as delivery material for transport of bioactive compounds and drugs in microcapsules and nanoparticles [6–8] and carrier material of beads for the immobilization of enzymes [9]. These uses are related to the filmogenic and rheological properties which can be tuned by the molecular weight (M_W) of Ch [8,10].

Ch is obtained by alkaline deacetylation of chitin, and consists of units of β-(1→4)-*N*-acetyl-2-amino-2-deoxy-D-glucose and β-(1→4)-2-amino-2-deoxy-D-glucose. This polysaccharide contains three types of reactive functional groups, an amino group ($–NH_2$) and both primary and secondary hydroxyl (–OH) groups at C-2, C-3 and C-6 positions, respectively. The amino group is able to react with aldehydes and ketones to give Schiff bases, as centers for acetylation, quaternizing alkylation, and metal chelation, etc.; while hydroxyl groups can give O-acetylation reactions, hydrogen bridges with polar atoms, etc. [11]. As well as chitin is insoluble in many organic solvents and in aqueous solutions, Ch is soluble as fully polycation in acid solutions, because the amino group has $pK_a = 6.3$ [12]. The optimal solubilization of Ch is achieved using formic, acetic and hydrochloric acids; but it is insoluble in sulfuric and phosphoric acids [13], indicating that Ch solubility is also affected by ionic strength and subsequent salting out effect.

Therefore, if it is pretended the use of these polysaccharides in aqueous media in a wide pH range, the improvement of solubilization of these materials is a mandatory goal. A common strategy for this goal is the incorporation of water-soluble functional groups such as glucosamine (GA) in the polymer chain of Ch through Maillard reaction (MR) [14–16]. The MR not only improves the solubility of the

modified polysaccharides, but also preserves their global properties and enhances their capabilities as delivery material in biological systems. Consequently, the determination of M_W and deacetylation degree (DD) is essential in modified Ch, since the amount of protons needed to solubilize the polysaccharide is equivalent to the present $–NH_2$ groups.

Among all biological properties of Ch, those related with antioxidant and antimicrobial activities are of utmost importance by the direct impact at biological and cellular levels [3,17–19]. Regarding this, the radical scavenging and metal ion-chelating capacity of Ch have been extensively studied, especially against different radical species [16,20,21] such as 1,1-diphenyl-2-picrylhydrazyl (DPPH) radical, peroxide radicals ($ROO^{\bullet}$), hydroxyl radical ($HO^{\bullet}$), superoxide radical ($O_2^{\bullet-}$), alkyl radical or preventing Fenton reaction [22,23]. The antioxidant activities for Ch were comparable to those obtained with commercial antioxidants, and the correlation of antioxidant activity with DD suggested that the pendant $–NH_2$ groups of Ch play a role in free radical scavenging activity probably by forming stable macromolecule radicals [24]. Nevertheless, to the best of our knowledge, the ability of Ch to deactivate singlet molecular oxygen ($^1O_2$) has been understudied, taking into account the relevance of this reactive species in oxidative processes at biological level [25].

On the other hand, antimicrobial activity of Ch has been attributed to the following properties: binding of Ch with anionic macromolecules of the cellular wall [26,27], interaction with cell membrane altering its permeability [28]; chelation of essential nutrients needed for growth [29] and/or binding with DNA inside the cell, inhibiting messenger RNA and protein synthesis [30]. However, the expression of this biological activity is limited by the intrinsic low solubility of Ch; hence, evaluation of antimicrobial properties of soluble Ch derivatives is also of great impact.

Currently, it is pursued to obtain biocompatible materials with single or multiple functionalities that can contribute to the enhancement of biological properties of bioactive compounds [31, 32]. The aims of this study were the synthesis by one-step/one-pot MR of both low and medium M_W Ch with glucosamine to obtain new water-soluble Ch derivatives (WSCh), and the characterization of their

physicochemical (MW, DD, solubility, structure) properties, $^1O_2$ quenching capability, and antibacterial activity against pathogenic microorganisms.

2. Materials and methods

2.1. Materials

Low and medium M_W Ch, e.g. (ChL) and (ChM), respectively, glucosamine hydrochloride (GA), tris(bipyridine)ruthenium(II) dichloride ($Ru(bpy)_3Cl_2$), tetradeuteroacetic acid (AA-d_4), furfuryl alcohol (FFA) and deuterium oxide (D_2O) were obtained from Sigma-Aldrich (MO, USA). Analytical grade monobasic potassium phosphate, ascorbic acid, hydrochloric acid (HCl), sodium hydroxide (NaOH), sodium chloride (NaCl) and sodium acetate (CH_3COONa) were obtained from Cicarelli (Buenos Aires, Argentina). Pullulan narrow standards (P-82, standard) were obtained from Showa Denko K.K. (Tokyo, Japan). Aqueous solutions were prepared with ultrapure water. *Staphylococcus aureus* (ATCC 6538), *Escherichia coli* (ATCC 35218), *Listeria ivanovii* (ATCC 19119), and *Enterococcus faecalis* (ATCC 29212) were obtained from the American Type Culture Collection (ATCC) and *Salmonella sp.* (LM006) was obtained from the Universidad Nacional de Río Cuarto collection center (Río Cuarto, Córdoba, Argentina). Mueller-Hinton Agar (MHA) and Nutritive Broth (NB) were purchased from Britania (Buenos Aires, Argentina).

2.2. Synthesis and physico-chemical characterization

2.2.1. Modification of Ch by Maillard reaction with glucosamine. WSCh derivatives were obtained by MR between ChL or ChM with GA according to the methodology proposed by Chung, Kuo and Chen (2005) [14], but with some modifications. Briefly, ChL or ChM (1% w/v) dissolved in 0.25 M CH_3COOH (pH 3), was mixed with GA (1% w/v), the reaction mixture was kept in an orbital shaker in an oven at 65 °C for 48 h. The derivatization reaction was monitored by UV-Vis absorption changes in the solution, using a UV-Vis diode array spectrophotometer (Analytik Jena model Specord S600). Once the reaction period was completed, the sample was centrifuged with a Thermo Scientific Sorval LST 16R centrifuge, at 5000 rpm during 20 min. The supernatant was

dialyzed against distilled water through a dialysis membrane with M_W cutoff of 12 – 14 kDa (Sigma-Aldrich) during 96 h at 4 ºC and then freeze-drying (Lyophilizer L-T8 RIFICOR).

2.2.2. Determination of deacetylation degree. Quantification of DD in both native and modified Ch was performed following the method proposed by Balázs and Sipos (2007) [33]. Aliquots of 0.1 g of native Ch and WSCh derivatives samples were dissolved in 100 mL of 0.01 M HCl solution, and small aliquots of a concentrated NaCl solution were added to keep constant the ionic strength to 0.1 M. A 20 mL aliquot was titrated with 0.1 N NaOH previously standardized using a pH meter (HI 2211, HANNA) for pH measurements. The titration curve was completed when a pH = 12 was reached and it showed two inflection points. The volume difference between both inflection values is the net volume of NaOH required to calculate the number of $–NH_2$ groups in the sample. The DD was calculated as follows (eqs. 1-3):

$$\text{DD}\,(\%) = x/(x+y)\ \times 100 \qquad (1)$$

with

$$x = \text{mol}\ (-\text{NH}_2)/w_{\text{sample}} = \Delta V_{\text{NaOH}} \times C_{\text{NaOH}}/w_{\text{sample}} \qquad (2)$$

$$y = \text{mol}\ (-\text{NHCOCH}_3)/w_{\text{sample}} = ((1-x)\times 161)/204 \qquad (3)$$

where w_{sample} is the weight of native Ch or WSCh, C_{NaOH} is NaOH molar concentration, 161 g mol^{-1} and 204 g mol^{-1} are the M_W of GA and acetylglucosamine, respectively.

2.2.3. Determination of the molecular weight. High Performance Liquid Chromatography–Size Exclusion Chromatography (HPLC–SEC) was used to obtain the chromatographic profile and average M_W of both native Ch and WSCh samples [34]. In all cases, 1.0 mg/mL solutions of polysaccharide samples were prepared by direct dissolution in buffer 0.5 M CH_3COOH/0.5 M CH_3COONa, pH 4.50. The acetate buffers used for dissolution were directly taken from the mobile phase reservoir used for SEC. The samples were filtered with a syringe filter containing a membrane of 0.45 μm pore size and 13 mm in diameter (GHP Acrodisc GF). Analyses were performed at room temperature with the buffer solution as mobile phase, at a flow rate of 0.8 mL/min, with sample

injection volume of 200 μL. The chromatographic system consisted of a binary pump (Waters, model 1525), and a set of five fractionation columns (Waters Ultrahydrogel, 7.8 mm × 300 mm each, and pore size of 120, 250, 500, 1000, 2000 Å, respectively). The fractionation limits of the columns were: 5×103, 8×104, 4×105, 1×106, and 7×106 g/mol, respectively. Detection was carried out with a differential refractometer (Waters, model 410), operated at 30 °C. All SEC data were acquired with the Breeze GPC software (Waters, Corp.), and then processed with Matlab^{TM} software (MathWorks, Inc.).

The chromatograph was calibrated with the set of Pullulan narrow standards. To this effect, individual solutions of each standard were prepared in the mobile phase at concentrations ca. 1 mg/mL, then filtered through a 0.45 μm filter and, finally, injected by duplicate. A linear calibration plot was obtained by least squared regression of the log of the peak M_W versus the peak elution volume (V) of all measured standards. Samples were injected by triplicate (n=3). The average M_W of each injected sample was obtained by combining its measured chromatograms with log M (V).

2.2.4. Determination of solubility at physiological pH. Previously dried 0.05 g of native Ch and their respective WSCh derivatives were dissolved in 5 mL of phosphate buffer pH 7.40 and shaken during 5 h at 25 °C [14]. Afterwards, samples were passed through a membrane filter of 0.22 μm pore size which was dried in an oven at 95 °C until constant weight. Solubility was estimated from the change in filter-paper weight [35]. The solubility was expressed in both (g/L) and (% w/w).

2.2.5. Fourier-Transform Infrared (FT-IR) Spectroscopy. The molecular structure of WSCh derivatives was analyzed by FT-IR by comparing with the structures of the respective native Ch. FT-IR spectra were recorded in the middle infrared (4000 cm^{-1} to 400 cm^{-1}) with a resolution of 2 cm^{-1} for 20 accumulations at room temperature in a spectrometer Nicolet model Nexus, with a cadmium mercury telluride (MCT) detector. Samples were prepared by grinding the dry WSCh derivatives or native Ch samples with KBr in a ratio 1:100 (1 mg sample: 100 mg KBr) and then compressed to form discs.

2.2.6. Quenching of Singlet Molecular Oxygen. Photosensitized generation and transient phosphorescence detection of $^1O_2$ were performed as previously described Giménez et al. (2016) [36]. Briefly, 57 μM $Ru(bpy)_3Cl_2$ dissolved in air-saturated D_2O solutions containing 0.1 M acetate buffer (pD 4.8 or 5.7) was excited with laser pulses at 355 nm (10 ns fwhm, 3 mJ/pulse) obtained with a ND:YAG laser Minilite II (Continuum, Santa Clara, CA). The transient phosphorescence signal of $^1O_2$, was detected at right angle from the laser beam through a bandpass filter at 1270 nm with a Peltier-cooled Ge photodiode J16TE2-66G (Teledyne Judson Technology, Montgomeryville, PA). The transient phosphorescence decay was fitted to a first-order decay law with eq. 4, with I_0 as the initial phosphorescence intensity and τ_Δ as the observed decay time of $^1O_2$.

$$I_{(t)} = I_0 \times \exp(-t / \tau_\Delta) \qquad (4)$$

In presence of a quencher molecule (Q), $^1O_2$ is deactivated through chemical reaction (k_r) and physical or collisional (k_p) parallel pathways, eqs. 5 and 6.

$$^1O_2 + Q \xrightarrow{k_r} \text{Oxidation products} \qquad (5)$$

$$^1O_2 + Q \xrightarrow{k_p} {}^3O_2 + Q \qquad (6)$$

In the present case, the interaction of $^1O_2$ with both native and WSCh samples (i.e. Q) was analyzed according to eq. 7, where the decreases of τ_Δ with the concentration of Q allows the calculation of the rate constant value for the total quenching of $^1O_2$ by Ch and WSCh samples ($k_t = k_r + k_p$), where $\tau_{\Delta,0}$ represents the lifetime of $^1O_2$ in the absence of Q.

$$\tau_\Delta^{-1} = \tau_{\Delta,0}^{-1} + k_t [Q] \qquad (7)$$

In turn, independent calculation of k_r was determined with eq. 8, by measuring the initial rate (v_0) of up-take of dissolved ground state oxygen $^3O_2$ as consequence of the reaction of $^1O_2$ with native Ch and WSCh samples and comparing with v_0 value obtained for a reference compound with known k_r, such as FAA with $k_r^{FAA} = 1.2 \times 10^8$ $M^{-1}s^{-1}$ [37].

$$k_r = k_r^{FFA} \frac{v_0^Q}{v_0^{FFA}} \frac{[FFA]_0}{[Q]_0} \quad (8)$$

The up-take kinetics of $^3O_2$ were performed by measuring the consumption of dissolved oxygen with a stainless-steel 1/16" FOXY-R-AF fiber-optic luminescent sensor of $^3O_2$ coupled to a CCD USB2000 fluorimeter (OceanOptics, Dunedin, FL). The sensor was placed on top of a sealed 5×5 mm path quartz cuvette (Hellma) containing 57 μM $Ru(bpy)_3Cl_2$ together with the respective $^1O_2$ scavenger (e.g. Ch derivatives or FAA) in 0.1 M acetate buffer solution (pH 4.7 or 5.8). A high power blue LED (462 ± 27 nm, 1 W) was used for selective excitation of the sensitizer $Ru(bpy)_3Cl_2$ (57 μM). Under those illumination conditions the fraction of light absorbed by the sensitizer was >97%, due to the tiny inner filter effect produced by the tail of the absorbance band of Ch's in the illuminated spectral region (Figure S1, Supplementary Information). Simultaneously, the absorbance spectral changes of the solution were also registered with an extra CCD-USB2000 spectrometer (OceanOptics), with the analyzing UV-Vis beam at right angle to the photolysis beam from the blue LED.

2.3. Biological experiments

2.3.1. Antimicrobial activity. The antibacterial assays were performed according to standard CLSI methods for antimicrobial dilution susceptibility tests [38]. The minimum inhibitory concentration (MIC) values against Gram positive bacteria *S. aureus* ATCC 6538, *E. faecalis* ATCC 29212, *L. ivanovii* ATCC 19119 and Gram negative bacteria *E. coli* ATCC 35218, *Salmonella sp.* LM006 were determined. The agar plate method was used to determine the MIC of native Ch and their respective WSCh derivatives samples. 1 % (w/v) solutions of samples were prepared in 1 % (v/v) acetic acid. NB prepared in 0.1 M acetate buffer pH 5.0 and 0.1 M phosphate buffer pH 7.4 was used. The Ch and WSCh samples were added to NB and then serially diluted by two-fold to give a final concentration of 0.1 %, 0.05 %, 0.025 %, 0.0125 %, 0.00625 % and 0.003125 % (w/v) in a 96-well plate. A standard 0.5 McFarland suspension (1–2×10^8 CFU/mL) was further diluted 10 fold so as to achieve a final test concentration of bacteria at approximately 1×10^7 CFU/mL per well in the

microtiter plate. A positive control was performed by inoculating a well without the addition of Ch or WSCh solutions to evaluate the effect of medium pH onto bacteria growth. A negative control with 0.1 % (w/v) of Ch or WSCh was used as sterile control. The microtiter plates were incubated at 37 ºC for 18 h. For MIC measurements, an aliquot of each dilutions and controls were plated on MHA and incubated at 37 ºC for 18 h. The MIC was determined as the lowest concentration of sample that achieved a 99.9 % decrease of viable cells.

The MIC was determined at pH 5.0 and 7.4, in order to evaluate the effect of protonation degree (polycationic character) and solubility of samples on the antimicrobial activity.

2.4. Statistical analysis

All the experiments were performed at 25 ºC by triplicate and data were presented as mean value ± standard deviation (SD). Kinetic experimental data were processed and analyzed with OriginPro 8.5® of OriginLab Software Corporation.

3. Results and discussion

3.1. Spectroscopic characterization of modified chitosans

The progress of the derivatization reaction of ChL and ChM samples by MR with GA was analyzed by both UV-Vis absorption and FT-IR spectroscopies. To confirm that ChL and ChM were not capable of self-reaction, Ch samples in the absence of GA were also subjected to the same reaction conditions. Fig. 1 compares the UV-Vis absorption spectra observed after 48 h of heating at 65 °C of ChM in 0.25 M CH3COOH (pH 3) solutions without and with the addition of 1% (w/v) GA, respectively. In the absence of GA, the absorption spectrum of ChM (solid line) does not change during the heating, as confirmed the constant value for the absorbance ratio between 275 nm and 350 nm (A_{275}/ A_{350}) shown in the inset of Fig. 1. On the other hand, in presence of GA the formation of a new sharp band at 275 nm was observed (dotted line), indicating the formation of colorless compounds during heating. In this case, the fast growth of the A_{275}/A_{350} ratio confirms that those transparent compounds were almost completely formed after 40 h of reaction. Nevertheless, dialysis of the latter heated solution through a membrane with cutoff at 12−14 kDa, produced the

disappearance of the sharp band at 275 nm, and the absorption spectrum of the remained solution (dash-dotted line) was closer to that for the parent polysaccharide. Moreover, no strong absorption band with maximum around 420 nm was developed, which is usually associated to the formation of unwanted brown melanoidin or hydroxymethylfurfural derivatives [38]. Hence, after 48 h of heating, almost the complete modification of the parent Ch was produced, with the releases of colorless compounds of low M_W (<12 kDa), probably produced by the breakdown of the polysaccharide chain. Similar results were also observed during the heating of low M_W Ch (ChL) (data not shown).

Figure 1.

Fig. 2 compares the FT-IR absorption spectra obtained in the region between 4000 and 400 cm^{-1} for the parent and modified low (a) and (b) medium M_W Ch's, respectively. The main effect of the MR on the FT-IR spectra is the absorbance enhancement of the characteristic vibrational bands of the Ch, in particular those at 3480 – 3440 cm^{-1}, 3260 – 3270 and 2960 – 2878 cm^{-1} corresponding to the characteristic O–H, N–H and C–H stretching regions. The higher intensity of the band at 3394 cm^{-1}, depicts a larger availability of –OH groups, strongly linked to the native molecules [16]. The increase in the shoulder at 3276 cm^{-1} responds to enlargement of stretching N–H of $–NH_2$ groups, denoting greater accessibility to such functional groups. The absorption bands at 1644, 1560 and 1320 cm^{-1} were assigned to amide I, II and III mode bands, respectively, while the characteristic bands of saccharide structure appeared at around 1155 cm^{-1} (anti-symmetric stretching of the C–O–C bridge), 1080 and 1034 cm^{-1} (skeletal vibrations involving the C–O stretching) [39]. The increases in the band 1636 cm^{-1} confirms the formation of –C=N bonds, characteristic of Schiff bases produced during non-enzymatic browning reactions, as intermediary compound [40]. In both modified Ch samples, a greater availability of (N–H) groups corresponding to the peptide bond (-acetylglucosamine) band at 560 cm^{-1} was observed. The strong increase of the band at 1100 cm^{-1} indicates conformational changes (modification in the vibration) of the pyranose structure, faithful to the addition of sugar molecules (branch) in the native polymer.

Thereby as from FT-IR spectral analysis, the MR between Ch and GA is demonstrated, yielding modified Ch with increased branching of the backbone of Ch and greater accessibility of principal's reactive groups of the molecule.

Figure 2

3.2. Deacetylation degree and molecular weight

Table 1 collects the DD values evaluated by titration with 0.1 N NaOH as indicated in Experimental section (see also Figure S2 of Supplementary Information). Data reported indicate that after derivatization of both ChL and ChM samples a reduction of about 10 % and 15 % on DD was produced, respectively. This effect can be attributed to the hydrolytic nature of the MR [41].

The chromatographic profiles obtained by HPLC-SEC indicated that both modified Ch showed higher retention times than the parent polysaccharide, as it is illustrated for ChL in Fig. 3a. From the molecular weight distribution (M_WDs) shown for native ChL and their respective derivative in Fig. 3b, the corresponding weight-average molecular weights (M_W) were obtained (Table 1). The results of Table 1 confirm that the M_W of the modified Ch samples were about six-time smaller than the respective native Ch's, confirming the hydrolytic breakdown of the polysaccharide chain during the Maillard reaction. Gullón et al. (2016) [42] obtained similar result, for the reaction between Ch with glucose under similar experimental conditions than in the present case (e.g. 2% (w/v) of Ch, 2% (w/v) of glucose at 60 °C and 32 h of reaction time).

Figure 3

Table 1

3.3. Solubility at physiological pH

The solubility of both modified Ch at pH 7.40 was significantly higher than the respective native Ch samples (Table 1). The solubility increase was parallel to the reduction of M_W of the polysaccharides. This result can be attributed to the decrease of hydrophobic intermolecular interactions, such as van der Waals forces, which favors polymer aggregation [43]. The same result

has been reported for other derivatization reactions of Ch with mono and disaccharides, resulting in the solubility increases in water [15].

3.4. Quenching of Singlet Molecular Oxygen ($^1O_2$)

Singlet molecular oxygen $^1O_2$ in solution is easily generated by photosensitization, through energy-transfer quenching mechanism of the excited triplet state of the photosensitizer by ground state molecular oxygen $^1O_2$ [36]. In polar solvent solutions, the coordination complex $[Ru(bpy)_3]^{2+}$ is a suitable photosensitizer with quantum yield generation of $^1O_2$ about 0.3-0.5 [36,44]. Absorption spectra of $[Ru(bpy)_3]^{2+}$ and Ch's mixtures were completely additive (data not shown), suggesting that no ground state interactions between the sensitizer and the polysaccharides were occurring. Laser pulsed excitation at 355 nm of $[Ru(bpy)_3]^{2+}$ in air-saturated D_2O solutions (pD 4.8 or 5.7) generates the transient phosphorescence signal of $^1O_2$ with a lifetime τ_Δ = 55-65 μs, as typically found in D_2O media [45] (inset of Fig. 4a). Upon the addition of Ch samples, the phosphorescence decay of $^1O_2$ become faster without changes of the initial phosphorescence intensity I_0. In the absence of sensitizer, control experiments done with laser excitation at 355 nm of the Ch samples in D_2O solutions did not generated $^1O_2$ (Figure S3 of supplementary Information). Thus, it can be expected that $^1O_2$ was only generated by the sensitizer and the polysaccharides deactivate it through a dynamic quenching mechanism as depicted in eqs. 5 and 6, and without interaction with the excited state of $[Ru(bpy)_3]^{2+}$ [35]. Hence, a linear dependence of τ_Δ^{-1} with the concentration of the polysaccharides is expected, eq. 7, yielding the global rate constant quenching k_t (= k_r+k_p) from the slope values of these plots (Fig. 4a). The k_t data in Table 2 correlated with the respective DD values of the polysaccharides (Table 1), indicating a relationship between efficiency of quenching of $^1O_2$ with the presence of $-NH_2$ groups in the polysaccharides [25]. In addition, the k_t values of Table 2 are more than three-order of magnitudes larger than the value of a primary amine molecule with similar structure than glucosamine, such as cyclohexylamine ($k_t = 8\times10^4$ $M^{-1}s^{-1}$) [46]. Hence, it can be expected that each polysaccharide molecule contributes with the deactivation of more than1000 molecules of $^1O_2$. In fact, the k_t values for the native ChL and ChM roughly correlated with the number of glucosamine

moieties in the polysaccharide chain, *e.g.* ≈1600 and 2800, respectively. However, for the WSCh derivatives the estimated number of glucosamine residues is ≈240 and 380 for WSChL and WSChM, respectively, suggesting that the increment of k_t in the WSCh derivatives can be associated with the presence of new moieties produced after the MR, which are more efficient quenchers of $^1O_2$.

Figure 4

Table 2

Fig. 4b shows the kinetic curves for the $^3O_2$-uptake in presence of Ch and WSCh samples and the reference compound FFA upon steady-state excitation of $[Ru(bpy)_3]^{2+}$ with the blue-LED in air-saturated 0.1 M acetate buffer solutions at pH 4.8. As mentioned before, the primary internal filter effect due to the blue-LED absorption by the chitosan samples was negligible (*e.g.* <3%) and therefore secondary $^3O_2$-uptake by direct excitation of chitosan can be ruled out [46,47]. The comparison of the initial rate value (v_0) of $^3O_2$-consumption by the samples and FFA with eq. 8 allowed the calculation of the rate constant for reactive quenching (k_r) for the $^1O_2$-mediated oxidation of the Ch derivatives, eq. 5. The results collected in Table 2 depict that the k_r values for the modified Ch are lower than for the respective native polysaccharide, indicating the improvement of the physical quenching pathway and decreasing the chemical degradation of the soluble Ch, as denotes the lower value of k_r/k_t (Table 2). The pH increment from 4.8 to 5.7 resulted in almost 50 % increases of both k_t and k_r. The pK_a values of the amine groups in Ch samples are ranging between 6.5 and 6.7 [4], hence, at pH 4.8 the amine groups are fully protonated (*e.g.* $–NH_3^+$), while at pH 5.7 only 30-35 % of $–NH_2$ groups can be expected. As the quenching mechanism of $^1O_2$ by amines is electron-transfer mediated [48,49], and the amine groups are easily oxidized than the ammonium species [50,51], both physical and chemical quenching of $^1O_2$ by the Ch are modulated by the protonation degree of the $–NH_2$ groups.

3.5. Antimicrobial activity

The antimicrobial activity of Ch can stem from various mechanisms, such as, binding at cell wall with change in cell membrane permeability [26-28], chelation of essential nutrients [29] and by inhibiting messenger RNA, protein synthesis and binding with DNA by cell penetration [30]. The antimicrobial effect has been shown to be dependent on the M_W of the polysaccharide [28], DD of Ch [50] and, especially, the host microorganism [16].

Table 3 collects the minimum inhibitory concentration (MIC) for the Ch and WSCh samples against both Gram positive and Gram negative pathogens at pH 5.0 and 7.4. The respective control of each experiment showed no bacteria growth inhibition by the culture media (pH effect), therefore the antimicrobial activity is only associated to Ch and WSCh samples.

Both native Ch and WSCh derivatives samples present ability to inhibit the growth of all tested bacteria showing better inhibitory effect at pH 5.0 than 7.4. This result is associated with the protonation of the $–NH_2$ groups and the positive global charge of the polysaccharide at acidic pH that increases the interaction with microorganism cell surface and the formation of impermeable layer around the cell wall.

The antimicrobial activity of WSCh derivatives compared to their respective parent native Ch was preserved against *Salmonella* sp. The same effect was observed with ChL and WSChL and *L. ivanovii*. whereas WSCh derivatives exhibit lower antimicrobial activity against *E. coli*, *E. faecalis* and *S. aureus*; this behavior can be the result of the decrease of DD in derivatives (about 12 %, Table 1) [17]. A marked tendency of antimicrobial effect with M_W reduction of samples was not observed. Additionally, all Ch samples showed the non-specific antibacterial activity against Gram-positive and Gram-negative microorganisms. Chung et al. 2005 [13] have evaluated the MIC values of a WSCh derivative obtained by MR between 1% (w/v) Ch (M_W 30-50 kDa and DD 90%) and 1 % (w/v) GA at 65 ºC for 2 day, against *E. coli* and *S. aureus* at pH 5.0 and 7.0. They found a larger antimicrobial activity for the WSCh than the respective native Ch. Hence, the combination of M_W and DD% already plays a role in the final antimicrobial activity of the polysaccharide, since both factors control the total amount of $–NH_2$ groups.

The MIC values reported in the present work were similar to those reported for others WSCh prepared also by MR with GA (heating at 50 ºC during 5 days and at 70 ºC at 3 days), obtaining MIC values of 0.025 % (w/v) against pathogens such as *S. aureus*, *Listeria monocytogenes*, *Bacillus cereus*, *E. coli*, *Shigella dysenteriae*, and *Salmonella typhimurium* at pH 5 and 7.0 [53].

Table 3

4. Conclusion

In this work, WSCh were prepared using Maillard reaction of glucosamine with low and medium M_W Ch p–without formation of undesired toxic melanoidin brown pigments. Under our experimental conditions, the solubility of the modified Ch increased about six-times relative to the native polysaccharide. The physicochemical characterization indicated that the reaction products have lower M_W and DD. Both native and modified Ch were able to quench singlet molecular oxygen $^1O_2$ with similar efficiency, being the quenching larger as the pH increased, due to the fractional increment of deprotonated amine groups ($-NH_2$).

The opposite pH effect was observed for the antimicrobial activity, since all studied Ch were more efficient antimicrobials at acidic than at neutral pH, reflecting the strong dependence on the protonation degree (polycationic character) of the samples. This behavior dependence is important because the protonated polymer could act as an antimicrobial against pathogenic microorganisms under pH conditions of the gastrointestinal tract.

In summary, the WSCh derivatives obtained in this work showed similar or enhanced antioxidant and antibacterial activities than the respective native Ch, but with a much larger aqueous solubility favoring their potential applications as bioactive compounds carrier materials for nutraceutical purposes.

ACKNOWLEDGMENTS

We thank Prof. Dr. G. G. Montich (Centro de Investigaciones en Química Biológica de Cordoba, Argentina) for collaboration in the analysis of molecular structures by Fourier Transform Infrared Spectroscopy (FT-IR), and Dr. R. A. Mignone (INBIONATEC) for technical assistance. This work has been supported in part by the Consejo Nacional de Investigaciones Científicas y Técnicas de Argentina (CONICET) grants PIP-2012-0374 and PIO20320150100052CO 2015-2016. Agencia de Promoción Científica y Tecnológica de Argentina (ANPCyT) grants PICT2012-266 and PICT 3444/14. N.V.B thanks CONICET for doctoral research fellowships. F.M.V., C.D.B., J.R.V., S.G.C. and M.A.M are research members of CONICET. M.M.Y is technical support staff of CONICET.

REFERENCES

[1] N. Lin, J. Huang, A. Dufresne, Preparation, properties and applications of polysaccharide nanocrystals in advanced functional nanomaterials: a review, Nanoscale. 4 (2012) 3274–3294.

[2] M.N. Ravi Kumar, A review of chitin and chitosan applications, React. Funct. Polym. 46 (2000) 1–27.

[3] I. Aranaz, M. Mengibar, R. Harris, I. Panos, B. Miralles, N. Acosta, G. Galed, A. Heras, Functional characterization of chitin and chitosan, Curr. Chem. Biol. 3 (2009) 203–230.

[4] Q.Z. Wang, X.G. Chen, N. Liu, S.X. Wang, C.S. Liu, X.H. Meng, C.G. Liu, Protonation constants of chitosan with different molecular weight and degree of deacetylation, Carbohydr. Polym. 65 (2006) 194–201.

[5] D.N. Ngo, M.M. Kim, S.K. Kim, Chitin oligosaccharides inhibit oxidative stress in live cells, Carbohydr. Polym. 74 (2008) 228–234.

[6] K.G.H. Desai, H.J. Park, Preparation and characterization of drug-loaded chitosan-tripolyphosphate microspheres by spray drying, Drug Dev. Res. 64 (2005) 114–128.

[7] R. Harris, E. Lecumberri, I. Mateos-Aparicio, M. Mengíbar, A. Heras, Chitosan nanoparticles and microspheres for the encapsulation of natural antioxidants extracted from Ilex paraguariensis, Carbohydr. Polym. 84 (2011) 803–806.

[8] B.N. Estevinho, F. Rocha, L. Santos, A. Alves, Microencapsulation with chitosan by spray drying for industry applications-A review, Trends Food Sci. Technol. 31 (2013) 138–155.

[9] B. Krajewska, Application of chitin- and chitosan-based materials for enzyme immobilizations: a review, Enzyme Microb. Technol. 35 (2004) 126–139.

[10] V.R. Sinha, A.K. Singla, S. Wadhawan, R. Kaushik, R. Kumria, K. Bansal, S. Dhawan, Chitosan microspheres as a potential carrier for drugs, Int. J. Pharm. 274 (2004) 1–33.

[11] V.K. Mourya, N.N. Inamdar, Chitosan-modifications and applications: opportunities galore, React. Funct. Polym. 68 (2008) 1013–1051.

[12] C.K.S. Pillai, W. Paul, C.P. Sharma, Chitin and chitosan polymers: chemistry, solubility and

fiber formation, Prog. Polym. Sci. 34 (2009) 641–678.

[13] M. Rinaudo, G. Pavlov, J. Desbrières, Influence of acetic acid concentration on the solubilization of chitosan, Polymer (Guildf). 40 (1999) 7029–7032.

[14] Y.C. Chung, C.L. Kuo, C.C. Chen, Preparation and important functional properties of water-soluble chitosan produced through Maillard reaction, Bioresour. Technol. 96 (2005) 1473–1482.

[15] Y.C. Chung, C.F. Tsai, C.F. Li, Preparation and characterization of water-soluble chitosan produced by Maillard reaction, Fish. Sci. 72 (2006) 1096–1103.

[16] G.Q. Ying, W.Y. Xiong, H. Wang, Y. Sun, H.Z. Liu, Preparation, water solubility and antioxidant activity of branched-chain chitosan derivatives, Carbohydr. Polym. 83 (2011) 1787–1796.

[17] R.C. Goy, D. De Britto, O.B.G. Assis, A review of the antimicrobial activity of chitosan, Polimeros. 19 (2009) 241–247.

[18] M. Dash, F. Chiellini, R.M. Ottenbrite, E. Chiellini, Chitosan-A versatile semi-synthetic polymer in biomedical applications, Prog. Polym. Sci. 36 (2011) 981–1014.

[19] W. Xia, P. Liu, J. Zhang, J. Chen, Biological activities of chitosan and chitooligosaccharides, Food Hydrocoll. 25 (2011) 170–179.

[20] J.Y. Je, S.K. Kim, Reactive oxygen species scavenging activity of aminoderivatized chitosan with different degree of deacetylation, Bioorganic Med. Chem. 14 (2006)

[21] H. Ai, F. Wang, Y. Xia, X. Chen, C. Lei, Antioxidant, antifungal and antiviral activities of chitosan from the larvae of housefly, *Musca domestica* L., Food Chem. 132 (2012) 493–498.

[22] R. Xing, S. Liu, Z. Guo, H. Yu, P. Wang, C. Li, Z. Li, P. Li, Relevance of molecular weight of chitosan and its derivatives and their antioxidant activities in vitro., Bioorg. Med. Chem. 13 (2005) 1573–1577.

[23] M.T. Yen, J.H. Yang, J.L. Mau, Antioxidant properties of chitosan from crab shells, Carbohydr. Polym. 74 (2008) 840–844.

[24] W. Xie, P. Xu, Q. Liu, Antioxidant activity of water-soluble chitosan derivatives, Bioorganic Med. Chem. Lett. 11 (2001) 1699–1701.

[25] G. V. Ferrari, M.E. Andrada, J. Natera, V.A. Muñoz, M. Paulina Montãna, C. Gambetta, M.L. Boiero, M.A. Montenegro, W.A. Massad, N.A. García, The employment of a removable chitosan-derivatized polymeric sensitizer in the photooxidation of polyhydroxylated water-pollutants, Photochem. Photobiol. 90 (2014) 1251–1256.

[26] B.K. Choi, K.Y. Kim, Y.J. Yoo, S.J. Oh, J.H. Choi, C.Y. Kim, *In vitro* antimicrobial activity of a chitooligosaccharide mixture against *Actinobacillus actinomycetemcomitans* and *Streptococcus mutans*, Int. J. Antimicrob. Agents. 18 (2001) 553–557.

[27] P. Eaton, J.C. Fernandes, E. Pereira, M.E. Pintado, F. Xavier Malcata, Atomic force microscopy study of the antibacterial effects of chitosans on *Escherichia coli* and *Staphylococcus aureus*, Ultramicroscopy. 108 (2008) 1128–1134.

[28] L.Y. Zheng, J.F. Zhu, Study on antimicrobial activity of chitosan with different molecular weights, Carbohydr. Polym. 54 (2003) 527–530.

[29] M. Kong, X.G. Chen, K. Xing, H.J. Park, Antimicrobial properties of chitosan and mode of action: a state of the art review, Int. J. Food Microbiol. 144 (2010) 51–63.

[30] N.R. Sudarshan, D.G. Hoover, D. Knorr, Antibacterial action of chitosan, Food Biotechnol. 6 (1992) 257–272.

[31] C. Caddeo, A. Nácher, O. Diez-Sales, M. Merino-Sanjuán, A. M. Fadda, M. Manconi, Chitosan-xanthan gum microparticle-based oral tablet for colon-targeted and sustained delivery of quercetin, J. Microencapsul. 2048 (2014) 1–6.

[32] P.L. Lam, R. Gambari, Advanced progress of microencapsulation technologies: *In vivo* and *in vitro* models for studying oral and transdermal drug deliveries, J. Control. Release. 178 (2014) 25–45.

[33] N. Balázs, P. Sipos, Limitations of pH-potentiometric titration for the determination of the degree of deacetylation of chitosan, Carbohydr. Res. 342 (2007) 124–130.

[34] A.I. Ruiz-Matute, A. Cardelle-Cobas, A.B. García-Bermejo, A. Montilla, A. Olano, N. Corzo, Synthesis, characterization and functional properties of galactosylated derivatives of chitosan through amide formation, Food Hydrocoll. 33 (2013) 245–255.

[35] M. Yalpani, L.D. Hall, Some chemical and analytical aspects of polysaccharide modifications. 3. Formation of branched-chain, soluble chitosan derivatives, Macromolecules. 17 (1984) 272–281.

[36] R.E. Giménez, V. Vargova, V. Rey, M.B.E. Turbay, I. Abatedaga, F.E. Moran Vieyra, V.I. Paz Zanini, J.H. Mecchia Ortiz, N.E. Katz, V. Ostatná, C.D. Borsarelli, Interaction of singlet oxygen with bovine serum albumin and the role of tryptophan residues and protein structure, Free Radic. Biol. Med. (2015).

[37] S.K. Allen, A. Todd, J.M. Allen, Photochemical formation of singlet molecular oxygen ($^1O_2$) in illuminated 6-methylcoumarin solutions, Biochem. Biophys. Res. Commun. 235 (1997) 615–618.

[38] CLSI, M07-A10: Methods for Dilution Antimicrobial Susceptibility Tests for Bacteria That Grow Aerobically; Approved Standard-Tenth Edition, 35 (2015) 1–87.

[39] M.R. Kasaai, A review of several reported procedures to determine the degree of N-acetylation for chitin and chitosan using infrared spectroscopy, Carbohydr. Polym. 71 (2008) 497–508.

[40] A.B. García-Bermejo, A. Cardelles-Cobas, A.I. Ruiz-Matute, F. Montañés, A. Olano, N. Corzo, Effect of drying methods on the reactivity of chitosan towards Maillard reaction, Food Hydrocoll. 29 (2012) 27–34.

[41] D.M. Bastos, É. Monaro, É. Siguemoto, M. Séfora, Maillard reaction products in processed food: pros and cons, in: B. Valdez (Ed.), Food Ind. Process.-Methods Equip., InTech, Rijeka, 2012: pp. 281–300.

[42] B. Gullón, M.I. Montenegro, A.I. Ruiz-Matute, A. Cardelle-Cobas, N. Corzo, M.E. Pintado, Synthesis , optimization and structural characterization of a chitosan – glucose derivative obtained by the Maillard reaction, Carbohydr. Polym. 137 (2016) 382–389.

[43] J. Li, Y. Du, H. Liang, Low molecular weight water-soluble chitosans: preparation with the aid of cellulase, characterization, and solubility, J. Appl. Polym. Sci. 102 (2006) 1098–1105.

[44] A.A. Abdel-Shafi, M.D. Ward, R. Schmidt, Mechanism of quenching by oxygen of the excited states of ruthenium (II) complexes in aqueous media. Solvent isotope effect and photosensitized generation of singlet oxygen, $O_2(^1\Delta_g)$, by $[Ru(diimine)(CN)_4]_2^-$ complex ions, Dalton Trans. (2007) 2517–2527.

[45] F. Wilkinson, J.G. Brummer, Rate constants for the decay and reactions of the lowest electronically excited singlet state of molecular oxygen in solution, J. Phys. Chem. Ref. Data. 24 (1995) 663–677.

[46] A. Sionkowska, A. Płanecka, K. Lewandowska, B. Kaczmarek, P. Szarszewska. Influence of UV-irradiation on molecular weight of chitosan. Progress on Chemistry and Application of Chitin and its Derivatives 18 (2013) 21-28.

[47] A. L. Andrady, A. Torikai, T. Kobatake. Spectral sensitivity of chitosan photodegradation. J. Applied Polym. Sci. 62 (1996) 1465-1471.

[48] R.H. Young, R.L. Martin, D. Feriozi, D. Brewer, R. Kayser, On the mechanism of quenching of singlet oxygen by amines-III. Evidence for a charge-transfer-like complex, Photochem. Photobiol. 17 (1973) 233–244.

[49] M.V. Encinas, E. Lemp, E.A. Lissi, Interaction of singlet oxygen $[O_2(^1\Delta_g)]$ with aliphatic amines and hydroxylamines, J. Chem. Soc. Perkin Trans. II. (1987) 1125–1127.

[50] A. Ray, A.F. Richter, A.G. MacDiarmid, A.J. Epstein, Polyaniline: protonation/deprotonation of amine and imine sites, Synth. Met. 29 (1989) 151–156.

[51] P. Darmanyan, A.P. Jenks, W.S. Jardon, Charge-transfer quenching of singlet oxygen $O_2(^1\Delta_g)$ by amines and aromatic hydrocarbons, J. Phys. Chem. 102 (1998) 7420–7426.

[52] Y. Omura, M. Shigemoto, T. Akiyama, H. Saimoto, Y. Shigemasa, I. Nakamura, T. Tsuchido, Antimicrobial activity of chitosan with different degrees of acetylation and molecular weights, Biocontrol Sci. 8 (2003) 25–30.

[53] Y.C. Chung, J.Y. Yeh, C.F. Tsai, Antibacterial characteristics and activity of water-soluble chitosan derivatives prepared by the Maillard reaction, Molecules. 16 (2011) 8504–8514.

Tables.

Table 1. Degree of deacetylation (DD), molecular weights (M_W) and solubility values for samples of native Ch and WSCh derivatives.

Chitosan	DD (%)	M_w (kDa)	Solubility % (w/w)	Solubility (g/L)
ChL	89 ± 1	297 ±45	5 ± 1	0.56 ± 0.02
ChM	78 ± 1	583 ± 87	3 ± 1	0.26 ± 0.02
WSChL	79 ± 2	49 ± 7	29 ± 2	2.83 ± 0.05
WSChM	63 ± 1	98 ± 15	18 ± 2	1.38 ± 0.04

Each value is expressed as mean ± standard deviation (n = 3).

Table 2. Rate constant values for the total quenching k_t and reactive quenching k_r of $^1O_2$ by low and medium molecular weight (M_W) native Ch or WSCh.

Chitosan	$k_t/10^8$ $M^{-1}s^{-1}$		$k_r/10^8$ $M^{-1}s^{-1}$		k_r/k_t	
	pD 4.8	**pD 5.7**	**pH 4.8**	**pH 5.7**	**pH 4.8**	**pH 5.7**
ChL	2.3±0.3	3.5±0.1	1.1. ±0.6	3.4± 0.8	0.47	0.98
ChM	1.3±0.2	2.7±0.6	1.6 ± 0.7	1.8 ± 1.0	1.22	0.68
WSChL	1.2±0.1	2.5±0.7	0.3 ± 0.1	0.8 ± 0.7	0.24	0.31
WSChM	0.9±0.2	2.1±0.4	0.4 ± 0.2	1.1 ± 0.9	0.41	0.53

Each value is expressed as mean ± standard deviation (n = 3).

Table 3. Minimum inhibitory concentration (MIC) in (% w/v), of native Ch and WSCh derivative samples at pH 5.0 and 7.4.

Sample	pH	MIC (% w/v)				
		E. coli	***Salmonella sp.***	***E. faecalis***	***S. aureus***	***L. ivanovii***
ChL	5.0	0.0125	0.0125	0.0125	0.025	0.05
	7.4	> 0.1	> 0.1	> 0.1	> 0.1	> 0.1
ChM	5.0	0.025	0.025	0.0125	0.05	0.0125
	7.4	> 0.1	> 0.1	> 0.1	> 0.1	> 0.1
WSChL	5.0	0.05	0.0125	0.05	0.1	0.05
	7.4	> 0.1	> 0.1	> 0.1	> 0.1	0.1
WSChM	5.0	0.05	0.025	0.025	0.1	0.025
	7.4	> 0.1	> 0.1	> 0.1	> 0.1	0.1

Figure captions

Fig. 1. UV-Vis absorbance spectra of 1 mg/mL medium M_W Ch (ChM) after 48 h of heating at 65 °C in acetate buffer solution pH 5.7: alone (solid line); in the presence of glucosamine (1% w/v) (GA) (dotted line); and after dialysis of the latter solution (dash-dotted line). Inset: time evolution of the absorbance ratio value at 275 nm and 350 nm (A_{275}/A_{350}) for ChM alone (■); and in presence of GA (1% w/v) (●).

Fig. 2. FT-IR absorption spectra obtained for previously lyophilized low (**a**) and medium (**b**) M_W native Ch (dark spectra) and WSCh (light spectra) samples.

Fig. 3. HPLC–SEC profiles (**a**) and molecular weight distribution (M_WDs) (**b**) obtained from the analysis of previously lyophilized low M_W native Ch (ChL) (solid line) and their water-soluble derivative (WSChL) (dash dotted line).

Fig. 4. a) Dependence of $^1O_2$ – lifetime τ_Δ with the concentration of Ch and WSCh samples in air-saturated in D_2O (pD 4.8, 0.1 M acetate buffer): (■) ChL, (●) ChM, (□) WSChL, and (○) WSChM. Inset: phosphorescence transient signal of $^1O_2$ obtained by pulsed laser excitation at 355 nm of 57 μM $Ru(bpy)_3Cl_2$ in D_2O (pD 4.8, 0.1 M acetate buffer). **b**) Ground state oxygen uptake profiles produced by steady-state photolysis (LED excitation at 462 ± 27) nm of $Ru(bpy)_3Cl_2$ (57 μM) in solution in 0.1 M acetate buffer pH 4.8 in presence of 10, 5, 50 and 25 μM of ChL, ChM, WSChL and WSChM, respectively, and 500 μM furfuryl alcohol (FFA).

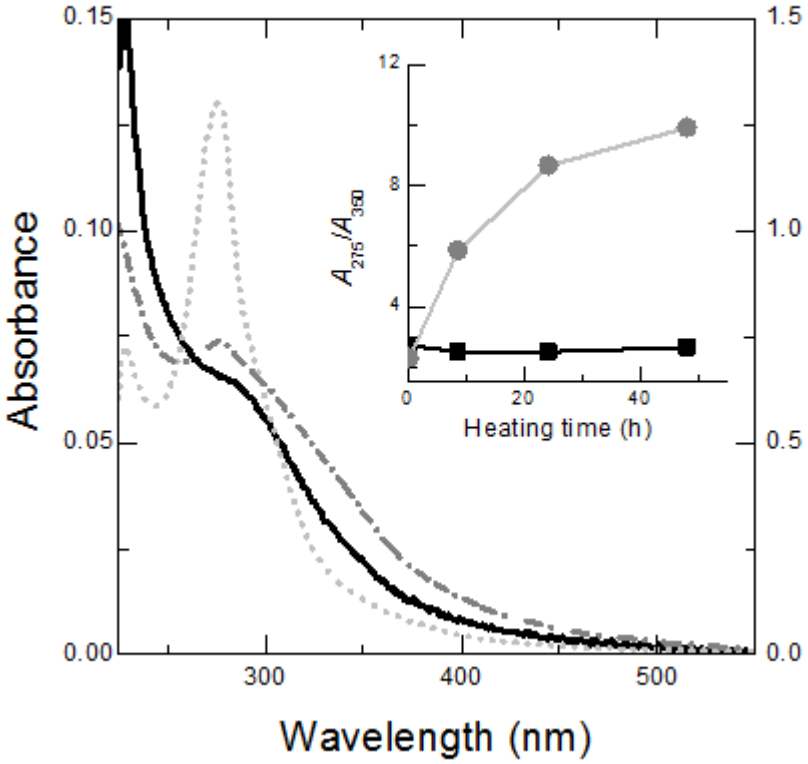

Figr-1

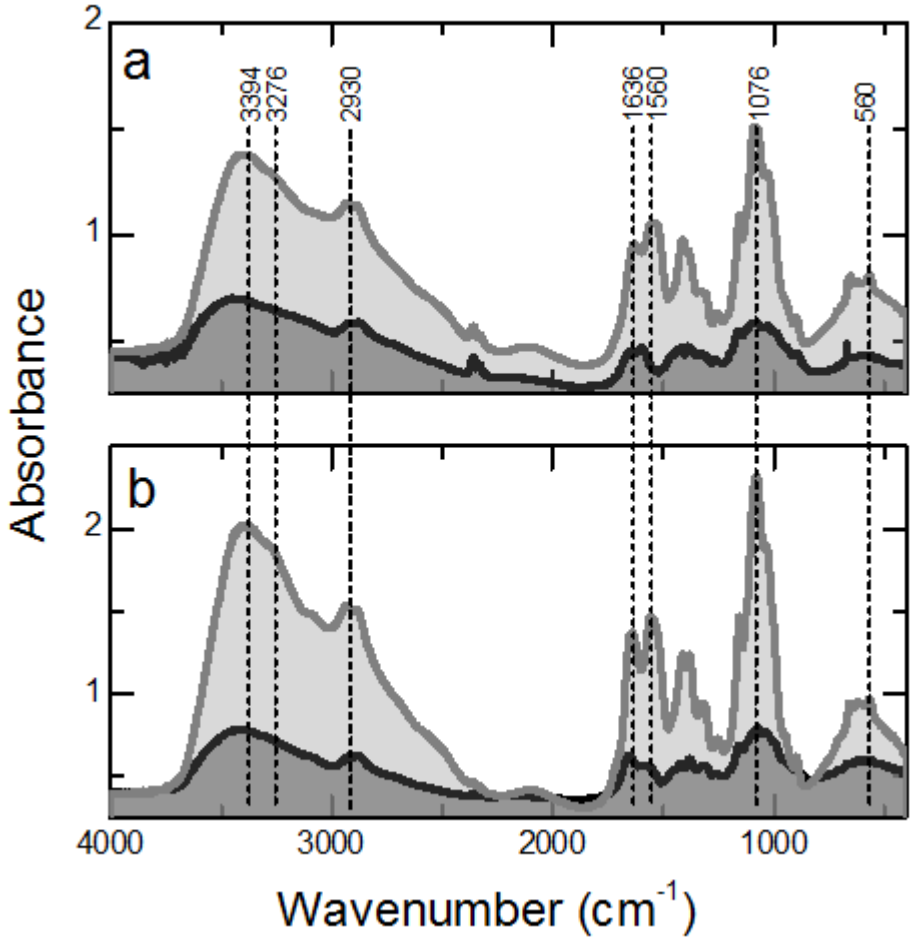

Figr-2

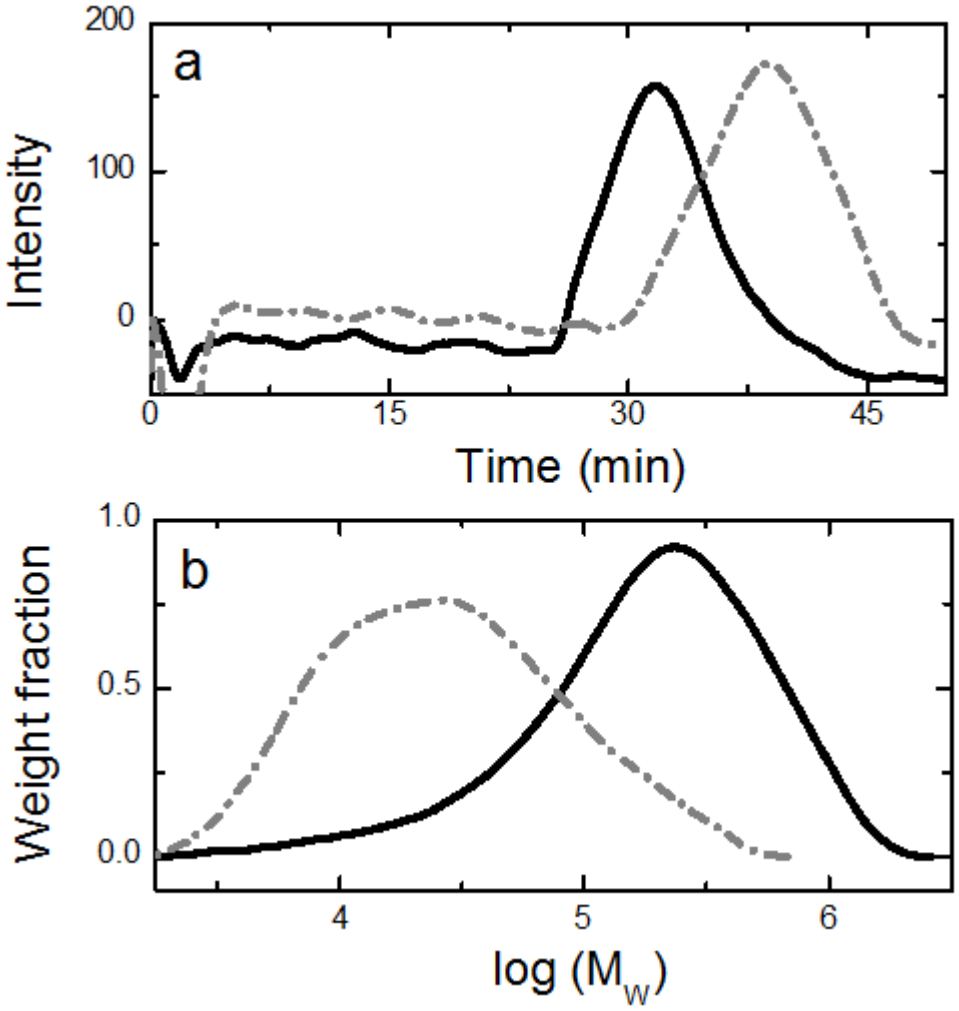

Figr-3

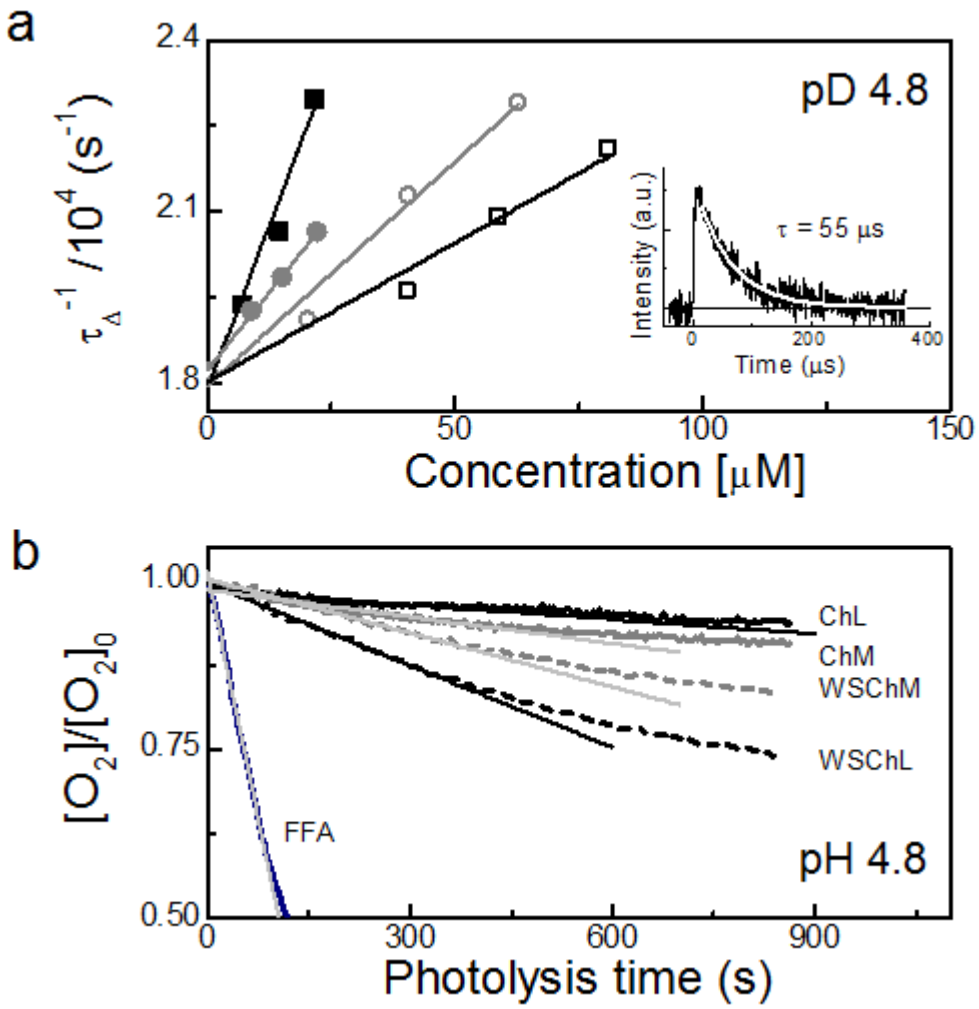

Figr-4